

**Synthesis and characterization of Sn-doped TiO<sub>2</sub> thin films for biosensor application**

M. Vanmathi<sup>a</sup>, A. Priya<sup>a</sup>, M. S. Tahir<sup>a</sup>, Sahir<sup>a</sup>, M. S. Razakh<sup>a</sup>, M. Senthil Kumar<sup>b,\*</sup>, R. Indrajit<sup>c</sup>, V. Elango<sup>d</sup>, G. Senguttuvan<sup>e</sup>, R V. Mangalaraja<sup>f</sup>

<sup>a</sup>*Department of Electronics and Communication Engineering, B. S. Abdur Rahman Crescent Institute of Science and Technology, Chennai, Tamil Nadu, India-600 048*

<sup>b</sup>*School of Mechanical Engineering, Vellore Institute of Technology, Chennai, Tamil Nadu, India-600 127*

<sup>c</sup>*Department of Physics, B. S. Abdur Rahman Crescent Institute of Science and Technology, Chennai, Tamil Nadu, India-600 048*

<sup>d</sup>*Department of Robotics and Automation, Easwari Engineering College, Chennai, Tamil Nadu, India-600 089*

<sup>e</sup>*Department of Physics, University College of Engineering, Anna University Tiruchirappalli, Tamil Nadu, India-621 316*

<sup>f</sup>*Department of Materials Science and Engineering, University of Adolfo Ibanez, Santiago, Chile*

TiO<sub>2</sub> a wide bandgap material has a great potential for use in semiconductor industry due to its better electronic properties combined with low cost, chemical stability and non-toxicity. Further metal doping is found to modify the conductivity, electrical, and optical characteristics. In this research, deposition of Sn-doped TiO<sub>2</sub> was carried out using the spray pyrolysis technique. The electrical properties were obtained by using the Hall effect technique and structural properties of the film were analyzed by X-ray diffraction and EDAX Scanning electron microscopy. The result of X-ray diffraction showed that the thin film deposited by spray pyrolysis is polycrystalline with preferential orientation in the direction of (002) fields. SEM analysis exhibited membrane structure for the thin film deposited by spray pyrolysis. The results of electrical conductivity were obtained by using the Hall effect technique.

(Received June 7, 2024; Accepted September 26, 2024)

**Keywords:** Titanium dioxide (TiO<sub>2</sub>), X-ray diffraction, Scanning electron microscopy (SEM), Hall effect

**1. Introduction**

Today, it is well known that the majority of semiconductors use titanium dioxide nanoparticles [1]. TiO<sub>2</sub> finds its application in sensors [2], antimicrobial agents [3], hydrogen [4], photo-catalysts [5], and the reduction of water evaporation [6]. TiO<sub>2</sub> is known for its good optical properties, inexpensive, non-toxic, and chemically stable.

Titanium dioxide (TiO<sub>2</sub>) a nanocrystalline materials has garnered significant attention due to its remarkable electrical and structural characteristics. TiO<sub>2</sub> is a Direct Band Gap Semiconductor (DMS) material with a band gap width of 3.24 eV [7] at room temperature, offering excellent chemical and thermal stability. Owing to their special electrical characteristics and sensitivity of sensors, wide band gap semiconductors are essential. Wide band gap semiconductors are susceptible to environmental changes, such as exposure to various gases. A wide band gap semiconductor's electrical characteristic, such its measured conductivity, can alter when it comes into contact with a sensing gas. Researchers are developing highly oriented TiO<sub>2</sub> thin films to leverage its opto-electronic properties in various applications like transparent electrodes for displays, window layers in solar cells, field emitters, ultraviolet laser emissions, photodetectors, and biosensors.

High working temperatures, poor selectivity, uneven repeatability, and instability are the limitations in TiO<sub>2</sub> use as gas sensors. Post-transition metals like aluminum (Al), gallium (Ga),

\*Corresponding author: msv305@yahoo.co.in  
<https://doi.org/10.15251/DJNB.2024.193.1345>

indium (In), tin (Sn), titanium (Ti), lead (Pb), and bismuth (Bi) offer favourable electrical and optical properties as sensor [8-12]. In particular, TiO<sub>2</sub> doped with Sn has been extensively researched and found to be an effective dopant. Tin (Sn) doping, in particular, enhances the electrical and optical characteristics of semiconductors like TiO<sub>2</sub>, exhibiting improved conductivity and optical absorption for diverse optoelectronic applications.

Deposition techniques, such as chemical vapor deposition [13], hydrothermal synthesis [14, 15], and sol-gel [16-19], are used to create Sn-doped TiO<sub>2</sub> thin films. Among the various techniques, Sol-gel remains an appropriate fabrication technique. Since the reactions were conducted in an aqueous solution, by modifying the pH level of the solution stops Ti<sup>4</sup> hydrolyzing. In summary, nanomaterials, especially nanocrystalline TiO<sub>2</sub> and Sn-doped TiO<sub>2</sub>, represent a significant area of research due to their unique properties and potential applications in electronic and photonic devices. Advancements in nanomaterial synthesis and characterization are crucial for unlocking their full potential in future technologies.

In this research, Sn-doped TiO<sub>2</sub> thin films deposition by Sol-gel technique is studied. As deposited samples were subjected to electrical and structural characterization.

## 2. Experimental procedure

The 8ml TTIP (Titanium Tetra Isopropoxide) is mixed with 40ml ethanol stirred for 15 minutes. To this solution 8ml of acetylacetone is added and stirred for another 15 minutes. Further, again 40ml of ethanol is added and stirred for 40 minutes. the required precursor TiO<sub>2</sub> solution is obtained. Stannous chloride (SnCl<sub>2</sub>) salt 7.5g taken is mixed with concentrated Hydrochloric acid and distilled water is added to the mixture. The solution is heated at 100° C for 1 hr. To the SnCl<sub>2</sub> solution, TiO<sub>2</sub> is added gradually and the solution is kept stirred continuously for 1 hr to obtain 2at% Sn doped TiO<sub>2</sub> solution.

The substrate is cleaned with deionized water and rinsed carefully and the excess water is wiped out. Next, the substrate is soaked in a chromic solution, which consists of ethanol and an IDP cleaning agent. It is then cleaned using distilled water and soap solution to remove the impurities. Finally, the substrate is cleaned and dried. The Sn-doped TiO<sub>2</sub> solution is sprayed on a clean glass substrate by spray pyrolysis technique. With the speed of 3500 RPM, for the duration of 30 seconds, the substrate (equal square size) is kept in the spin equipment and the vacuum is turned on to hold the substrate. The solution is added gradually to the substrate. The a spray rate of 4 ml/min, air as carrier gas, the pressure of 3 bar, at a substrate temperature of 350°C, nozzle to substrate distance of 15 cm is maintained. On depositing the solution on to the substrate, it is left for 5 hours to cool down. Finally, the thin film substrate is annealed for 1 hour at 350°C. The process of deposition is repeated for 7 times and the substrate is annealed for 1 hour at 350°C after each deposition process. The (model: Rigaku, Dltex ultra 250) powder diffracted meter recorded XRD pattern was obtained using CuK $\alpha$  radiation ( $k=1.5406 \text{ \AA}$ ) of Sn-doped ZnO thin films.

The Scanning Electron Microscope (SEM) was used to record the morphology of the thin films to investigate their microstructure. The resistivities were measured using a high resistivity meter at the room temperature.

## 3. Results and discussion

### 3.1. Resistivity measurement

It is possible to determine the concentration, mobility, and dependence of the charge carriers in your sample on temperature and magnetic field by combining resistivity and Hall effect measurements. The density of free carriers, or electrons or holes, has a significant impact on a semiconductor's electrical characteristics. Generally, a semiconductor's conductivity is increased through donor or acceptor concentration doping.

Fig. 1 shows the shows the electrical resistivity of the Sn doped substrate. The decrease graph shows that the substrate possesses low resistance and high electrical conductivity at different temperatures. It is well known that high resistivity samples make Hall effect measurements more

challenging. As the Hall voltage is usually a small percentage of the voltage drop that is used to calculate resistivity. Therefore, for the samples with the highest resistivity, particularly at low temperatures, that can be well observed from the results. Thus, when resistivity increases dramatically, reliable Hall measurements were not attainable. These factors prevents from using the current setup to get the complete set of temperature-dependent data in highest resistivity samples in terms of resistivity, carrier concentration and mobility. The results obtained from this research are consistent with the literature reported.

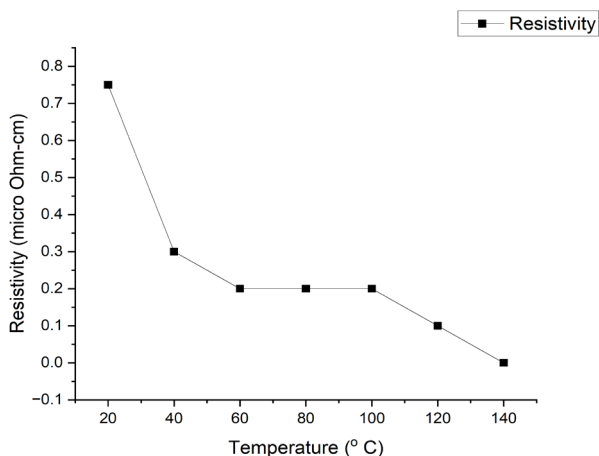


Fig. 1. Resistivity of substrate obtained by Hall effect.

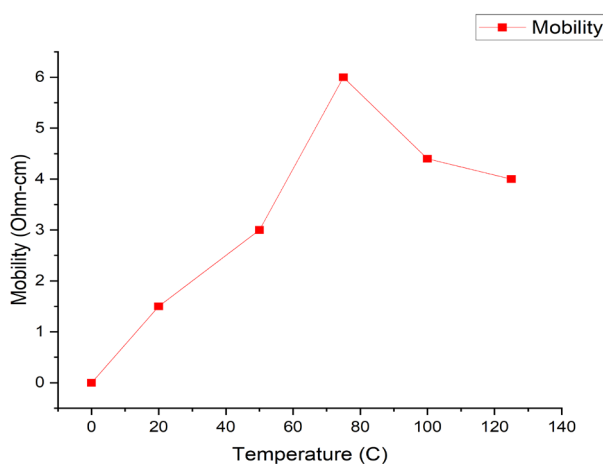


Fig. 2. Mobility of the substrate obtained by Hall effect.

Fig. 2 shows the movement of freely moving electrons on the substrate at different temperatures. The increase in the graph clearly shows the electron mobility on the substrate. The reason being, there are more charge carriers at higher temperatures. These carriers have greater energy, there are more collisions, mobility decreases with temperature.

The electron concentration of TiO<sub>2</sub> deposited on the substrate at different temperatures. The increasing graph shows the electrical conductivity of the substrate. The connection between the carrier concentration and the Si source temperature is exponential, as predicted by Fig. 3. The carrier concentration that was highest was attained by the thin film was in line with as previously noted by others [20]. The challenges in Sn doped TiO<sub>2</sub> cause the free carrier concentration that increase with increase in temperature. An electron concentration of  $6.43 \times 10^{-9} \Omega\text{-cm}^3$  obtained at a Si source temperature of 70°C.

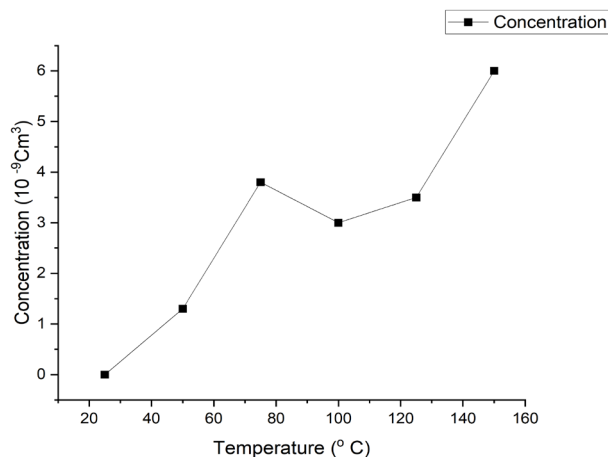


Fig. 3. Electron concentration of the substrate obtained by Hall effect.

### 3.2. Microstructural analysis

The result analysis was done for thin film deposition to find how well the doped material is coated on the substrate and to find the structure and orientation of the atoms. EDAX and FESEM are the common methods for finding the structural analysis and for finding orientations, arrangement and spacing of atoms XRD analysis is used.

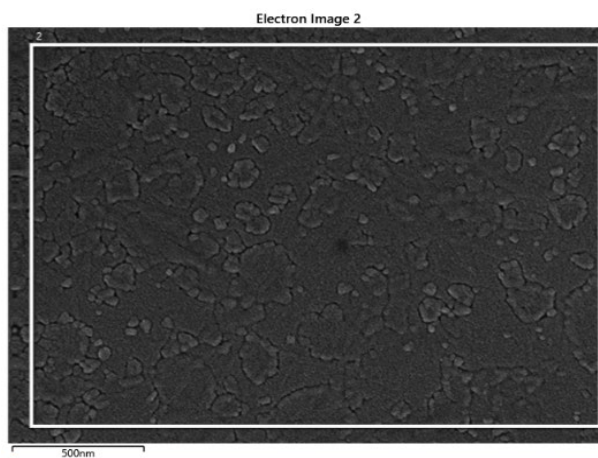


Fig. 4. SEM result of thin film deposited by spray pyrolysis.

Scanning Electron Microscopy result of thin film which is deposited by the spray pyrolysis technique is shown in fig. 4. It is observed that the structure of thin film deposited by spray pyrolysis was membrane structure which indicates the uniform coating of solution on the substrate. Thin film revealed a uniform homogeneous structure in terms of microstructure with better microstructure's density. The reason could be the addition of Sn dopant, that acts inhibits the grain growth, resulted in smaller grains [22]. The stress-induced disruption of grain growth caused by the difference in ionic radius between  $Zn^{2+}$  (0.074 nm) and  $Sn^{2+}$  (0.069 nm) cause the grain size obtained in the case of Sn doping to gradually decrease as the Sn doping concentration increases. The films' microstructure is made up of many grains that resemble rice that are evenly spaced over the surface. EDAX analysis is used to examine the film composition in Fig. 5, and various elements presence can be observed in the spectrum in Fig 6 and 7. This could be confirmed from the results shown in table 1.

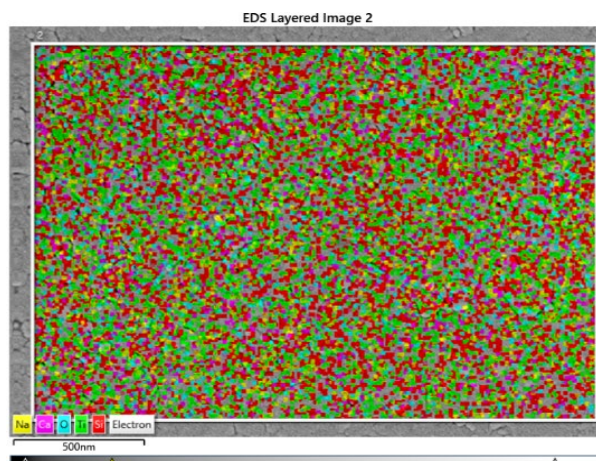


Fig. 5. EDS result of spray pyrolysis.

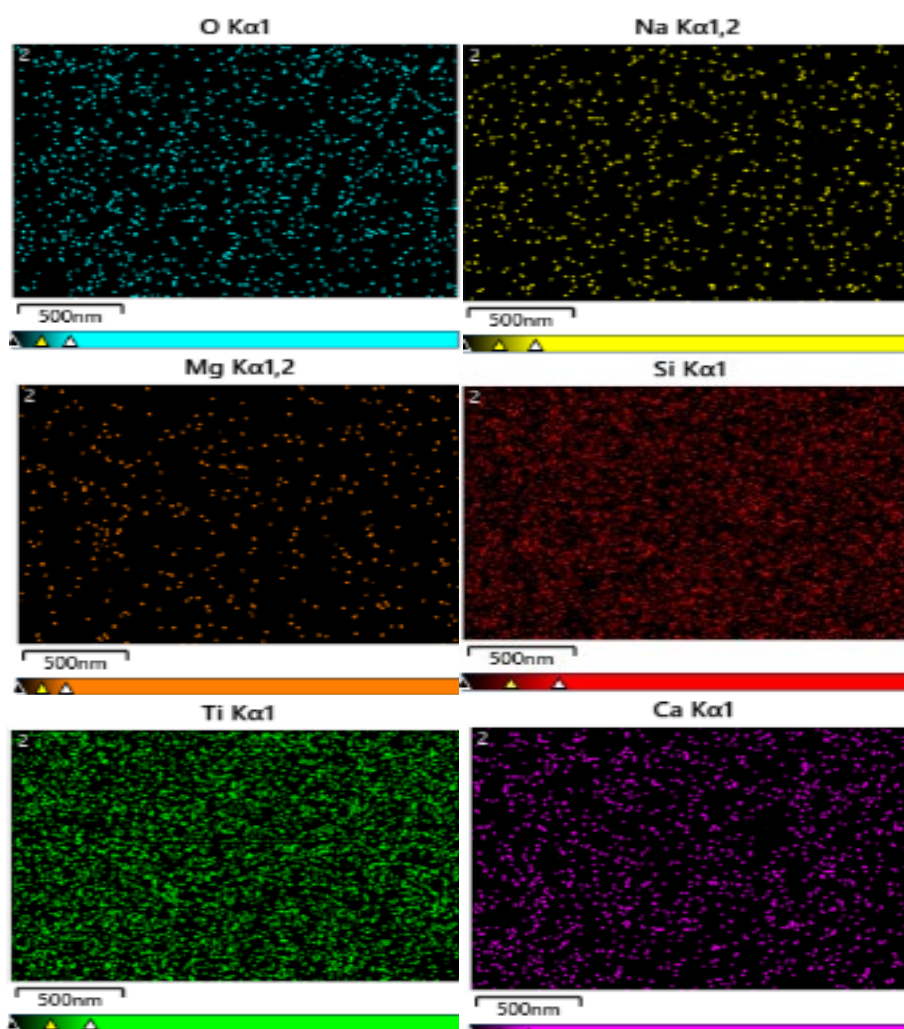


Fig. 6. Electron deposition of individual metals.

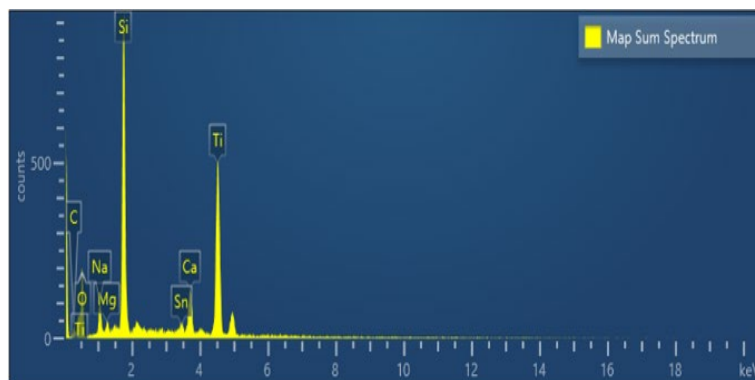


Fig. 7. EDAX result 2 of spray pyrolysis.

Table 1. Map sum spectrum of spray pyrolysis.

Map Sum Spectrum				
Element	Line Type	Weight %	Weight % Sigma	Atomic %
O	K series	36.76	1.33	56.45
Na	K series	4.46	0.34	4.76
Si	K series	22.48	0.59	19.67
Ca	K series	5.12	0.26	3.14
Ti	K series	31.17	0.79	15.99
Total		100.00		100.00

### 3.3. Structural analysis

Fig. 8 shows the XRD pattern of Sn doped TiO<sub>2</sub> thin film. It is observed that the intensity is high at an angle of around 25 degrees. It states that the structure is a polycrystalline structure with preferential orientation in the direction of 2 theta (002). These patterns line up with the (100), (002), and (101) principal diffraction peaks of crystalline ZnO. This result showed that the sn doped TiO<sub>2</sub> thin films had been annealed for one hour at 350 °C, resulted in polycrystalline films with a wurtzite structure that is hexagonal (JCPDS 36–1451).

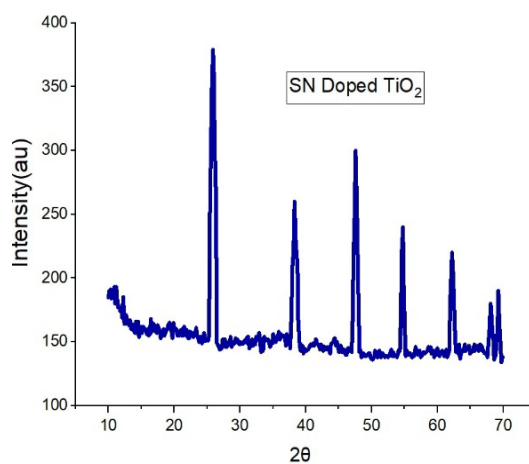


Fig. 8. XRD of TiO<sub>2</sub>.

The polycrystalline, hexagonal wurtzite structure was present in the XRD patterns t (100) plane. In the XRD patterns, there were secondary peaks linked to the ZnO structure's (002), (101),

and (103) planes [21]. The (100) peak intensity decreased dramatically and the secondary peaks nearly vanished as the doping was increased. For Sn doped films, the degree of preferential growth stayed the same along the (100) plane even when the severity of the preferential orientation decreased. In the Sn-doped TiO<sub>2</sub> samples, anatase and brookite were formed, while the only crystalline structure in the pure TiO<sub>2</sub> sample was anatase. The crystalline structure of TiO<sub>2</sub> incorporates the Sn<sup>4+</sup> ion. As the concentration of Sn<sup>4+</sup> rises, the brookite phase grows and the anatase phase declines.

#### 4. Conclusion

It is concluded that though the structure of the thin film deposited by the spin coating is platelet structure, the EDAX-FESEM results for the thin film deposited by spray pyrolysis overtake the advent. The EDAX result provides the sightful elemental contribution and dispersion on the sample. The Hall effect technique provides the concentration, mobility of electrons, and also the substrate resistance. Therefore, it concluded that a resistivity of 0.21 μΩ-cm, a mobility of 6.43 x 10<sup>-9</sup> Ω-cm<sup>3</sup> and a carrier concentration of 4 x 10<sup>-9</sup> Ω-cm<sup>3</sup> was obtained at room temperature. Also, from the results, with increase in temperature, the mobility decreases and increase in resistivity and carrier concentration was observed. The increasing concentration of TiO<sub>2</sub> electrons shows the conductivity property of the substrate and the result would be much enhanced in the case of substrate made of ITO.

#### References

- [1] J Buha, Applied surface science, 321, 457 (2014); <https://doi.org/10.1016/j.apsusc.2014.10.039>
- [2] J M Rzaizj, A M Abass, Journal of Chemical Reviews, 2, 114 (2020); <https://doi.org/10.33945/SAMI/JCR.2020.2.4>
- [3] M R Amiri, M Alavi, M Taran, D Kahrizi, Journal of Public Health Research, 11, 22799036221104151 (2022); <https://doi.org/10.1177/22799036221104151>
- [4] J. Cai, J Shen, X Zhang, Y H Ng, J Huang, W Guo, C Lin, Y Lai, Small Methods, 3, 1800184 (2019); <https://doi.org/10.1002/smt.201800184>
- [5] N T Padmanabhan, N Thomas, J Louis, DT Mathew, P Ganguly, H John, S C Pillai, A review. Chemosphere, 271, 129506 (2021); <https://doi.org/10.1016/j.chemosphere.2020.129506>
- [6] M Ghorbanpour, S Lotfiman, Micro & Nano Letters, 11, 648 (2016); <https://doi.org/10.1049/mnl.2016.0259>
- [7] Y Q Cao, T He, L S Zhao, E J Wang, W S Yang, Y A Cao, Journal of Physical Chemistry C, 113, 18121 (2009); <https://doi.org/10.1021/jp9069288>
- [8] O Carp, C L Huisman, A Reller, Progress in Solid State Chemistry, 32, 33 (2004); <https://doi.org/10.1016/j.progsolidstchem.2004.08.001>
- [9] A Kitiyanan, S Ngamsinlapasathian, S Pavasupree, S Yoshikawa, Journal of Solid State Chemistry, 178, 1044 (2005); <https://doi.org/10.1016/j.jssc.2004.12.043>
- [10] M D'urr, S Rosselli, A Yasuda, G Nelles, Journal of Physical Chemistry B, 110, 21899 (2006); <https://doi.org/10.1021/jp063857c>
- [11] J Li, H C Zeng, Journal of the American Chemical Society, 129, 15839 (2007); <https://doi.org/10.1021/ja073521w>
- [12] M. Vanmathi M Senthil Kumar, M. Mohamed Ismail, Senguttuvan.G, Materials Research Express 6, 106423 (2019); <https://doi.org/10.1088/2053-1591/ab3a02>
- [13] Y A Cao, W S Yang, W F Zhang, G Z Liu, P Yue, New Journal of Chemistry, 28, 218 (2004); <https://doi.org/10.1039/b306845e>

- [14] J Liu, Y Zhao, LY Shi et al., *Applied Materials & Interfaces*, 3, 1261 (2011); <https://doi.org/10.1021/am2000642>
- [15] E Arpac, F Sayılkan, M Asiltürk, P Tatar, N Kiraz, H Sayılkan, *Journal of Hazardous Materials*, 140, 69 (2007); <https://doi.org/10.1016/j.jhazmat.2006.06.057>
- [16] J Sun, X L Wang, J Y Sun, R X Sun, S P Sun, L P Qiao, *Journal of Molecular Catalysis A*, 260, 241 (2006); <https://doi.org/10.1016/j.molcata.2006.07.033>
- [17] X Li, R C Xiong, G Wei, *Journal of Hazardous Materials*, 164, 587 (2009); <https://doi.org/10.1016/j.jhazmat.2008.08.069>
- [18] L Q Jing, H G Fu, BQ. Wang et al., *Applied Catalysis B*, 62, 82 (2006).
- [19] S Mahanty, S Roy, S Sen, *Journal of Crystal Growth*, 261, 77 (2004); <https://doi.org/10.1016/j.jcrysgro.2003.09.023>
- [20] C.J. Eiting, P.A. Grudowshi, and R.D. Dupuis, *Journal of Electronic Materials*, 27, 206 (1998); <https://doi.org/10.1007/s11664-998-0388-5>
- [21] Chien-Yie Tsay, Hua-Chi Cheng, Yen-Ting Tung, Wei-Hsing Tuan, Chung-Kwei Lin a, *Thin Solid Films*, 517, 1032 (2008); <https://doi.org/10.1016/j.tsf.2008.06.030>
- [22] S Dhanapandian, A Arunachalam, C Manoharan, *Appl Nanosci.*, 6, 387 (2016); <https://doi.org/10.1007/s13204-015-0450-6>
- [23] X Wang, T Wang, G Si, Y Li, S Zhang, X Deng, X Xu, *Sens. Actuators B Chem.*, 302, 127165 (2020); <https://doi.org/10.1016/j.snb.2019.127165>